2013

Neurotropic arboviruses induce interferon regulatory factor 3-mediated neuronal responses that are cytoprotective, interferon independent, and inhibited by western equine encephalitis virus capsid

Daniel C. Peltier
University of Michigan Medical School
Helen M. Lazear
University of Michigan Medical School
Jocelyn R. Farmer
University of Michigan Medical School
Michael S. Diamond
Washington University School of Medicine in St. Louis
David J. Miller
University of Michigan Medical School

JVI Journals.ASM.org

Neurotropic Arboviruses Induce Interferon Regulatory Factor 3-Mediated Neuronal Responses That Are Cytoprotective, Interferon Independent, and Inhibited by Western Equine Encephalitis Virus Capsid

Daniel C. Peltier,[a] Helen M. Lazear,[a] Jocelyn R. Farmer,[a] Michael S. Diamond,[c,d,e] David J. Miller[a,b]

Departments of Microbiology and Immunology[a] and Internal Medicine,[b] University of Michigan Medical School, Ann Arbor, Michigan, USA; Departments of Medicine,[c] Molecular Microbiology,[d] and Pathology and Immunology,[e] Washington University School of Medicine, St. Louis, Missouri, USA

Cell-intrinsic innate immune responses mediated by the transcription factor interferon regulatory factor 3 (IRF-3) are often vital for early pathogen control, and effective responses in neurons may be crucial to prevent the irreversible loss of these critical central nervous system cells after infection with neurotropic pathogens. To investigate this hypothesis, we used targeted molecular and genetic approaches with cultured neurons to study cell-intrinsic host defense pathways primarily using the neurotropic alphavirus western equine encephalitis virus (WEEV). We found that WEEV activated IRF-3-mediated neuronal innate immune pathways in a replication-dependent manner, and abrogation of IRF-3 function enhanced virus-mediated injury by WEEV and the unrelated flavivirus St. Louis encephalitis virus. Furthermore, IRF-3-dependent neuronal protection from virus-mediated cytopathology occurred independently of autocrine or paracrine type I interferon activity. Despite being partially controlled by IRF-3-dependent signals, WEEV also disrupted antiviral responses by inhibiting pattern recognition receptor pathways. This antagonist activity was mapped to the WEEV capsid gene, which disrupted signal transduction downstream of IRF-3 activation and was independent of capsid-mediated inhibition of host macromolecular synthesis. Overall, these results indicate that innate immune pathways have important cytoprotective activity in neurons and contribute to limiting injury associated with infection by neurotropic arboviruses.

Neurotropic arthropod-borne viruses (arboviruses) preferentially infect neurons of the central nervous system (CNS) and belong to several different positive- and negative-sense RNA virus families. Clinically relevant neurotropic arboviruses include flaviviruses (e.g., West Nile virus [WNV], St. Louis encephalitis virus [SLEV], and Japanese encephalitis virus), bunyaviruses (e.g., La Crosse virus [LACV] and California encephalitis virus) and New World alphaviruses (e.g., eastern, western, and Venezuelan equine encephalitis viruses [EEEV, WEEV, and VEEV, respectively]). These pathogens cause endemic and epidemic viral encephalitis (1) and are emerging or reemerging in many areas of the world. At present, there are no effective treatments for these highly morbid and potentially lethal viral infections (2).

Cell-intrinsic innate immune responses are essential for pathogen control and cell survival after infection (3–8), and an effective response in neurons may be crucial to prevent irreversible loss of critical CNS neurons following neurotropic arbovirus infection. Innate immune responses are activated by pattern recognition receptors (PRRs) such as the transmembrane Toll-like receptors (TLR) and the cytoplasmic receptors retinoic acid inducible gene I (RIG-I) and melanoma differentiation-associated gene 5 (MDA5) (9). These receptors bind ligands containing pathogen-associated molecular patterns (PAMPs) such as modified carbohydrate, lipid, or nucleic acid structures (10, 11). Receptor ligation induces signal transduction cascades that result in the activation of the central PRR pathway transcription factors NF-κB, interferon regulatory factor 3 (IRF-3), and IRF-7 and the production of type I interferons (IFNs), proinflammatory cytokines, and other cellular factors that contribute to an antiviral microenvironment (11). In addition, PRR signaling is important for activating adaptive immune responses, which are required for clearance of many viral infections (12, 13). Thus, PRR-mediated pathways play a pivotal role in controlling viral infections, although the full complement of innate immune response functions has not been defined and remains an active area of investigation.

Due to differential pathway component expression, ligand specificity, and pathogen-mediated antagonism, PRRs respond to viral infections in a pathogen-specific manner (9, 14). Moreover, cell type-specific differences in PRR pathway responses are well documented and underscore the importance of studying innate immunity in key targeted cell types (15, 16). For example, plasmacytoid dendritic cells preferentially utilize TLR7, TLR9, and IRF-7 for innate recognition and signaling, whereas fibroblasts and conventional dendritic cells require RIG-I-like receptors and the IRF-3 pathway (17, 18). Within the CNS, IRF-3$^{-/-}$ cortical neurons differ in their basal expression of PRR components and responses to WNV compared to IRF-3$^{-/-}$ myeloid cells (3). In addition, the host defense response to WNV in cortical neurons is more dependent upon IRF-3 and IRF-7 than is the case for myeloid cells (6). These results suggest that neurons may have restricted innate immune capabilities, perhaps due in part to their unique and crucial physiologic functions and irreplaceable nature.

Neuronal innate immune function and its impact on neurotropic virus pathogenesis have not been fully defined, but im-

Received 12 October 2012 **Accepted** 19 November 2012
Published ahead of print 28 November 2012
Address correspondence to David J. Miller, milldavi@umich.edu.

doi:10.1128/JVI.02858-12

portant observations have been made. We and others have demonstrated that neurons possess active antiviral PRR pathways mediated by the receptors TLR3, RIG-I, and MDA5, which can activate NF-κB and IRF-3 and induce type I IFN production (19–25). In addition, neurons produce type I IFNs in response to infection by several neurotropic viruses (3, 5, 25–28), and WNV replication is enhanced in cortical neurons isolated from IPS-$1^{-/-}$, TLR3$^{-/-}$, IRF-3$^{-/-}$, and IRF-7$^{-/-}$ mice (3–6, 29). Furthermore, IRF-3$^{-/-}$ mice are more susceptible to intracranial but not intravenous inoculation of herpes simplex virus (HSV) (30), and humans deficient in TLR3 are predisposed to HSV encephalitis (31). Together, these observations provide strong evidence that neurons possess active and functional PRR-mediated pathways, which may be a critical determinant in neurotropic virus pathogenesis.

In this report, we used targeted genetic approaches in neurons derived from multiple sources to study PRR pathway activation and function in response to neurotropic arbovirus infection. In response to WEEV and SLEV infection, neurons activated an IRF-3-dependent prosurvival pathway, which was independent of type I IFN activity. Furthermore, PRR-mediated innate immune pathway signaling in neurons could be inhibited by WEEV capsid protein in a manner that was downstream of IRF-3 activation and independent of host translational shutoff. These results demonstrate that neurons have functional and beneficial innate immune pathways that are capable of responding to neurotropic viral infections yet remain susceptible to virus-encoded countermeasures, and they also identify key cellular determinants that may be exploited in the development of more efficacious vaccines and antiviral therapeutics.

MATERIALS AND METHODS

Mice. Wild-type C57BL/6 mice were obtained commercially (Jackson Laboratories, Bar Harbor, ME). IRF-3$^{-/-}$ and IFNAR$^{-/-}$ mice were obtained originally from T. Taniguchi (Tokyo, Japan) and J. Sprent (Scripps Institute, San Diego, CA), respectively, and backcrossed onto a C57BL/6 background. All mice were genotyped and bred in animal facilities of Washington University School of Medicine, and experiments were approved and performed in accordance with Washington University animal study guidelines.

Plasmids. The dominant negative (DN), superactive (SA), and wild-type overexpression plasmids pDN-IRF-3(ΔN), pSA-IRF-3(S396D), pSA-TRIF(ΔC), and pMDA5 and the secreted alkaline phosphatase (SEAP) promoter-reporter plasmids pISRE-SEAP and pNFκB-SEAP (ISRE is interferon-stimulated response element) were purchased from InvivoGen (San Diego, CA). The hemagglutinin (HA)-tagged β-galactosidase expression control plasmid pCMV-LacZ, also referred to as pIVT-LacZ, has been previously described (32). The WEEV replicon plasmid bearing a yellow fluorescent protein (YFP)-tagged, truncated capsid (pRep-YFP) has been previously described (33). WEEV and WNV protein expression plasmids were generated by inserting individual PCR-amplified viral genes initially into pMT/V5-HisA (Invitrogen, Carlsbad, CA) and subsequent subcloning into the final constitutive expression vector pCMV-TnT (Promega, Madison, WI). WEEV structural and nonstructural genes were amplified from the full-length cDNA clone pWE2000 (34), and WNV genes were amplified from the cDNA nonstructural protein clone pc-WNV (provided by Richard Kinney, CDC, Atlanta, GA). Primer sequences and detailed cloning procedures are available upon request.

Antibodies and reagents. Antibodies against the HA epitope tag, glyceraldehyde-3-phosphate dehydrogenase (GAPDH), IRF-3, MDA5, and WEEV have been previously described (24, 34, 35). Antibodies against actin and the V5 epitope tag were purchased from Sigma-Aldrich (St. Louis, MO), and antibodies against TRIF were generously provided by Marc Hershenson (University of Michigan, Ann Arbor, MI). Neutralizing antisera against mouse type I IFNs were purchased from PBL Biomedical Laboratories (Piscataway, NJ). All secondary antibodies for immunoblotting were purchased from Jackson ImmunoResearch (West Grove, PA).

Recombinant human IFN-α-A/D, human tumor necrosis factor (TNF)-α, and poly(I-C) have been previously described (24). Mouse IFN-α/β was obtained from the Biodefense and Emerging Infections (BEI) Research Resources Repository (Manassas, VA).

Viruses. The Cba 87 strain of WEEV was generated from the cDNA clone pWE2000 as previously described (34). For infection of primary rodent neurons and human embryonic stem cell (hESC)-derived neurons, we used sucrose gradient-purified WEEV. Vero cells were infected with WEEV at a low multiplicity of infection (MOI), harvested 48 h later, and centrifuged at 1,000 × *g* for 5 min to pellet cellular debris, and virions were precipitated from precleared tissue culture supernatant by addition of polyethylene glycol and sodium chloride to 7% and 2.3% final concentrations, respectively, and gentle stirring overnight at 4°C. Virions were recovered by centrifugation at 3,500 × *g* for 20 min, resuspended in Hanks' balanced salt solution (HBSS), loaded onto 15 to 45% linear sucrose step gradients, and centrifuged at 40,000 × *g* for 90 min. Visible virion bands were collected, diluted in HBSS, pelleted at 35,000 × *g* for 60 min, resuspended in HBSS, and stored at −80°C in single-use aliquots. To inactivate WEEV, we exposed culture supernatants or purified virions to UV light for 15 min on ice using a Spectrolinker cross-linker (Spectronics Corporation, Westbury, NY), which reproducibly blocked the propagation of infectious virions in Vero cells. Virus titers were determined by plaque assay on Vero cell monolayers as previously described (34).

SLEV strain TBH-23 and LACV strain LACV/human/1960 were obtained from Robert Tesh (University of Texas Medical Branch, Galveston, TX) and were propagated in Vero cells. Green fluorescent protein (GFP)-tagged Sendai virus (SeV) was obtained from Valery Grdzelishvili (University of North Carolina at Charlotte, Charlotte, NC) and has been previously described (24). All experiments with infectious WEEV or SLEV were performed under biosafety level 3 (BSL3) conditions in accordance with University of Michigan Institutional Biosafety Committee and CDC/NIH guidelines.

Cell culture. Human neuroblastoma [BE(2)-C], differentiated BE(2)-C/m, baby hamster kidney (BHK-21), and African green monkey kidney (Vero) cells were cultured as previously described (24, 34). BHK-21 cells stably expressing bacteriophage T7 RNA polymerase (BSR-T7 cells) (33) were cultured in Dulbecco's modified Eagle medium containing 10% fetal bovine serum, 0.1 mM nonessential amino acids, 10 U per ml penicillin, and 10 μg per ml streptomycin. BE(2)-C/m cells were transfected using Lipofectamine 2000 (Invitrogen) according to the manufacturer's instructions except that 25% of the recommended amount of DNA was used, which routinely resulted in 60 to 70% transfection efficiency (data not shown). BHK-21 and BSR-T7 cells were transfected using TransIT LT-1 (Mirus, Madison, WI) as previously described (33).

Primary rat cortical neurons were isolated and cultured as previously described (24). For primary mouse cortical neurons, cortices from embryonic day 15 mice were dissociated and cultured as described for rat cortical neurons (24) except that cells were plated at a density of 5×10^5 per cm^2 on poly-D-lysine- and laminin-coated plates and washed once 3 h after plating and medium was replenished every 1 to 2 days until cells were used for experiments after 10 to 12 days in culture. Cultured neurons were highly susceptible to glutamate-induced excitotoxicity (data not shown), a characteristic of differentiated cortical neurons (36).

Differentiated human neurons were derived from the NIH-approved hESC line H7 (WiCell, Madison, WI) through the sequential development of embryoid bodies, neuroepithelial rosettes, neuroprogenitor cells, and differentiated neurons based on modified procedures of previously published techniques (37–39) (J. Farmer and D. Miller, unpublished results).

Cell viability, SEAP assays, immunoblotting, and immunofluorescence microscopy analyses. Cell viability was determined by a 3-[4,5-dimethylthiazol-2-yl]-2,5-diphenyltetrazolium bromide (MTT) assay as

TABLE 1 RT-PCR primer sequences

Target	Primer ID	Sequence (5′ to 3′)
18S rRNA	rRNA-F	CTTAGAGGGACAAGTGGCG
	rRNA-R	ACGCTGAGCCAGTCAGTGTA
Human IFN-β	hIFNβ-F	TGGGAGGATTCTGCATTACC
	hIFNβ-R	CAGCATCTGCTGGTTGAAGA
Mouse IFN-β	mIFNβ-F	GCAGCTCCAGTTCCGACAAAG
	mIFNβ-R	GACCACCATCCAGGCATAGC
ISG15	hISG15-F	GCGGGCTGGAGGGTGTG
	hISG15-R	CCGCAGGCGCAGATTCAT
OASL	hOASL-F	CTGTTGCTATGACAACAGGGAG
	hOASL-R	CACGATGAGGTTGAAATCTGG
Viperin	hRSAD2-F	CGCCACAAAGAAGTGTCCTGC
	hRSAD2-R	CTACACCAACATCCAGGATGGACT
WEEV envelope glycoprotein 1	WEEV E1-F	TACGGGCACATCCCTATCTC
	WEEV E1-R	GTCGCTTCCTTCAAAACAGC

previously described (34) or a luminescent ATP assay (ATPlite; PerkinElmer, Waltham, MA) according to the manufacturer's instructions. SEAP assays, immunoblotting, and immunofluorescence microscopy were performed as previously described (24, 33, 34), except that immunofluorescence images were obtained with a Nikon Eclipse Ti microscope and images were processed with Nikon NIS Elements and Adobe Photoshop software.

RT-PCR analysis. Reverse transcription-PCR (RT-PCR) was performed as previously described (24, 33). For quantitative RT-PCR (qRT-PCR) analyses we normalized threshold values to 18S rRNA levels and determined fold increases using threshold cycle ($\Delta\Delta C_T$) calculations. RT-PCR primer sequences are shown in Table 1.

Protein synthesis and metabolic labeling. We used metabolic incorporation of ^{35}S-labeled methionine and cysteine to measure total protein synthesis. Control and WEEV-infected cells were incubated with 50 μCi per ml PRO-MIX ^{35}S-cell labeling mix (Amersham) for 30 min, washed with Tris-buffered saline containing 100 μg cycloheximide per ml, and lysed in SDS-PAGE sample buffer. Samples were separated by electrophoresis, and gels were fixed in a solution containing 25% methanol and 7% acetic acid, impregnated with 1 M sodium salicylate, dried under vacuum, and exposed to film at −80°C. Digitized images of radiolabeled protein bands were quantitated by densitometry as described previously (34).

Statistical analysis. We used a two-tailed Student's *t* test assuming unequal variances and considered a *P* value of <0.05 as statistically significant. Unless otherwise indicated, results are representative of at least three independent experiments, where quantitative data represent the mean ± standard error of the mean (SEM).

RESULTS

WEEV replication induces IFN-β transcription in neurons. The activation of innate immune pathways and transcriptional upregulation of type I IFN and other antiviral genes is a common characteristic of many viral infections. However, the full breadth of cell types that can activate these pathways, the individual viruses that efficiently stimulate them, and the viral-mediated countermeasures to antagonize their effects are not fully known. We have recently demonstrated that human neuronal cells possess functional innate immune pathways activated by several PRRs in response to both synthetic ligands and the potent innate immune system activator SeV (24). To examine this in the context of a more physiologically relevant neurotropic virus, we examined IFN-β transcriptional responses of cultured neuronal cells after infection with WEEV, a highly pathogenic and neurotropic alphavirus (Fig. 1). Both SeV and WEEV infection induced IFN-β mRNA accumulation in BE(2)-C/m cells (Fig. 1, left bars), which are differentiated human neuroblastoma cells with morphological and biochemical characteristics of mature human neurons in culture and have been used previously to study cellular responses to WEEV infection (34). Furthermore, UV-inactivated WEEV failed to potently stimulate IFN-β transcription in BE(2)-C/m cells (Fig. 1, black bar), suggesting that viral replication was required for full innate immune system activation. To examine whether WEEV infection upregulated IFN-β transcription in other neuronal cells, we also infected hESC-derived and primary rat cortical neurons with SeV or WEEV and measured IFN-β mRNA levels by qRT-PCR. Both SeV and WEEV induced IFN-β transcription in hESC-derived neurons (Fig. 1, middle bars) and primary rat cortical neurons (Fig. 1, right bars). Together, these results suggested that active WEEV infection induced an innate immune response in CNS neurons.

IRF-3 mediates a neuronal cytoprotective response against WEEV infection. The transcription factor IRF-3 is a central regulator of virus-induced innate immune system activation (11). Thus, we examined whether disruption of IRF-3 function in BE(2)-C/m neuronal cells would alter responses to WEEV infection (Fig. 2 and 3). We ectopically and stably expressed an IRF-3 dominant negative (dnIRF-3) mutant that lacks a DNA binding domain such that it competes for activation signals but does not induce transcription. This dnIRF-3 mutant potently suppresses PRR-mediated pathway activation induced by poly(I-C) and SeV in BE(2)-C/m cells (24). Expression of dnIRF-3 decreased the IFN-β transcriptional response to WEEV infection by >90% compared to control BE(2)-C/m cells transfected with empty vector (Fig. 2A). We also examined the effects of dnIRF-3 expression on WEEV-induced cytopathic effect (CPE) and infectious virion production in BE(2)-C/m cells. Virus-induced CPE is a hallmark of alphavirus infection in most cultured mammalian cells, including neurons, where the intensity of CPE often depends on cellular

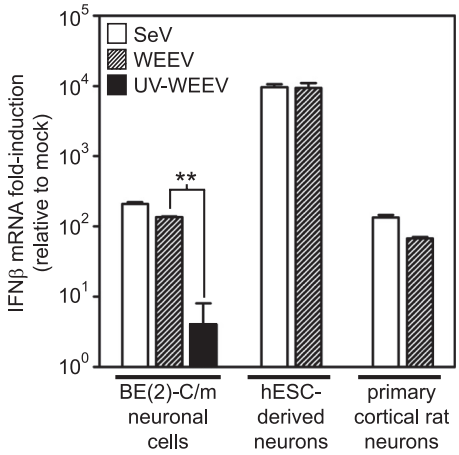

FIG 1 WEEV infection induces IFN-β transcription in cultured neurons. BE(2)-C/m cells, hESC-derived neurons, or primary rat cortical neurons were infected with SeV, infectious WEEV, or UV-inactivated WEEV, and IFN-β transcript levels were assessed via qRT-PCR. WEEV was used at an MOI of 1 for both BE(2)-C/m and primary rat neurons and an MOI of 0.1 for hESC-derived neurons, and qRT-PCR was done at 20 to 24 hpi. **, $P < 0.005$.

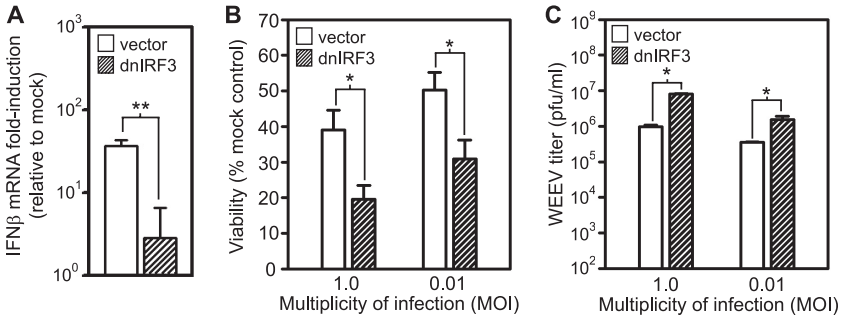

FIG 2 IRF-3 mediates IFN-β transcriptional induction, enhances neuronal survival, and suppresses infectious virion production in BE(2)-C/m cells in response to WEEV infection. (A) BE(2)-C/m cells stably expressing control vector or dnIRF-3 construct were mock infected or infected with WEEV at an MOI of 1 for 20 h, and IFN-β transcript levels were measured by qRT-PCR. (B and C) BE(2)-C/m cells expressing the vectors described in panel A were infected with WEEV at the indicated MOI and both the percent viability relative to mock-infected controls (B) and infectious viral titers in tissue culture supernatants (C) were measured at 48 hpi. Similar differences in viral titers were seen when tissue culture supernatants were examined at 20 hpi (data not shown).

differentiation (34, 40). Functional disruption of IRF-3 rendered BE(2)-C/m cells more susceptible to WEEV-induced CPE (Fig. 2B) and also increased infectious virus production by ~5- to 10-fold (Fig. 2C).

We further analyzed IRF-3-mediated protective responses in BE(2)-C/m cells, and the potential effects of viral inoculum on these responses, by infecting empty vector- or dnIRF-3-expressing cells with WEEV at various MOIs and analyzing the temporal pattern of cell survival over 72 h (Fig. 3A). At 12 hours postinfection (hpi) there was minimal WEEV-induced CPE in both empty vector- and dnIRF-3-expressing cells regardless of viral inoculum, despite the fact that >95% of cells in both groups infected with an MOI of 10 had detectable WEEV antigens at this time point (Fig. 3B). At lower inocula the percentage of WEEV-infected cells at 12 hpi decreased as expected but did not differ between empty vector- and dnIRF-3-expressing cells. Virus-induced CPE rapidly

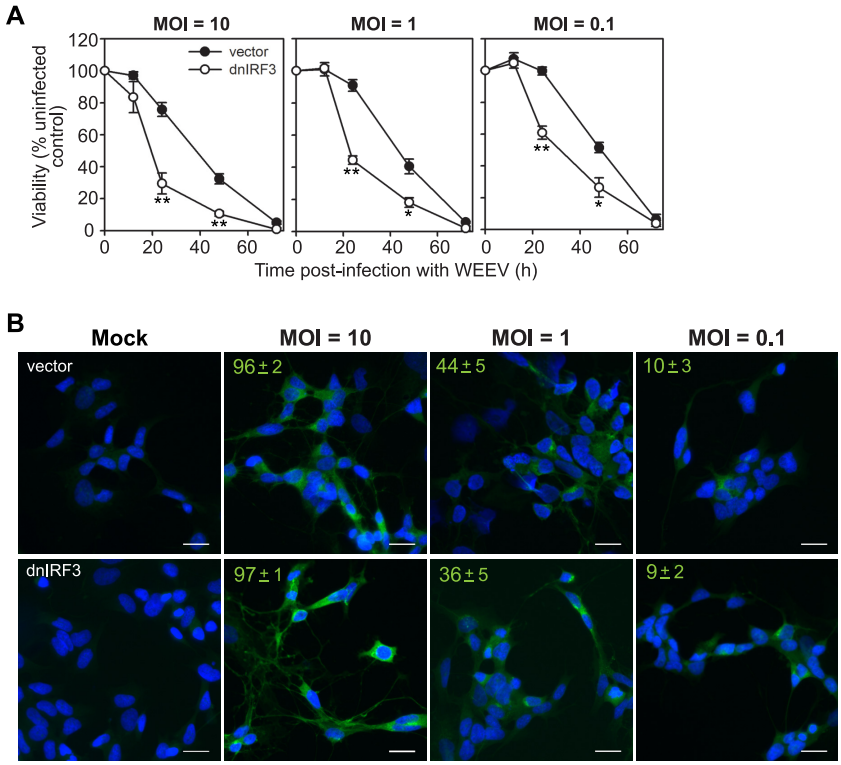

FIG 3 IRF-3 enhances neuronal survival in BE(2)-C/m cells in response to WEEV infection irrespective of viral inoculum. (A) BE(2)-C/m cells stably expressing control vector or dnIRF-3 construct were infected with WEEV at the indicated MOI and percent viability relative to mock-infected controls was measured from 12 to 72 hpi. *, $P < 0.05$; **, $P < 0.005$ (compared to WEEV-infected cells expressing control vector at the corresponding time point). (B) Immunofluorescence microscopy images of BE(2)-C/m cells stably expressing control vector (upper images) or dnIRF-3 construct (lower images) infected with WEEV at the indicated MOI and analyzed at 12 hpi. Representative overlaid images from one of two independent experiments are shown, where blue indicates 4′,6-diamidino-2-phenylindole (DAPI)-stained nuclei and green indicates WEEV-infected cells. We quantitated the percentage of infected cells by analyzing four separate fields obtained at ×20 magnification, which corresponded to enumerating ~250 cells per group. Values in the upper left corners indicate means ± standard deviations (SD) of the percentage of cells positive for WEEV antigens. Scale bars, 25 μm.

progressed in dnIRF-3-expressing cells such that a significant difference in viability compared to that of control cells was evident at both 24 and 48 hpi, whereas virus-induced cell death was virtually complete by 72 hpi in both groups (Fig. 3A). We cannot exclude the possibility that more rapid viral spread in culture due to enhanced infectious virus production in dnIRF-3-expressing cells (Fig. 2C) was responsible for the observed increase in CPE at lower MOIs. However, the results under high-MOI conditions, in which essentially all cells were infected (Fig. 3B), indicated that a cell intrinsic neuronal response mediated by IRF-3 was responsible for the cytoprotective effect.

In addition to loss-of-function studies with dnIRF-3, we conducted gain-of-function studies with ectopic expression of either wild-type or constitutively active IRF-3 in BE(2)-C/m cells. WEEV-mediated CPE and infectious viral titers were markedly suppressed in cells expressing either construct (data not shown). However, subsequent analyses revealed that ectopic expression of either wild-type or constitutively active IRF-3 in BE(2)-C/m cells resulted in the production of type I IFNs prior to infection, and we have previously demonstrated that exogenous type I IFNs have potent cytoprotective and antiviral effects in BE(2)-C/m cells (34). Thus, we could not reliably interpret the gain-of-function studies with respect to cell intrinsic innate immune responses.

To provide additional validation of IRF-3-mediated responses to WEEV infection in CNS neurons, we used primary cortical neurons derived from wild-type and IRF-3$^{-/-}$ mice (Fig. 4). The absence of IRF-3 reduced but did not eliminate WEEV-induced IFN-β transcriptional upregulation in cultured mouse neurons (Fig. 4A), suggesting that rodent neurons possess both IRF-3-dependent and -independent pathways to activate IFN-β transcription in response to neurotropic alphavirus infection, consistent with previous results obtained using WNV (3). The absence of IRF-3 also increased the susceptibility of mouse neurons to WEEV-mediated CPE (Fig. 4B), consistent with results using dnIRF-3 expression in human BE(2)-C/m neuronal cells (Fig. 2B and 3A). However, virus titers were not significantly increased in neuronal cultures from IRF-3$^{-/-}$ mice (Fig. 4C), in contrast to results with human neuronal cells (Fig. 2C), suggesting a potential species-specific difference in neuronal responses or a distinct effect of primary versus immortalized cells. Nevertheless, these results indicated that IRF-3 mediated a cytoprotective response in cultured neurons infected with WEEV. We chose to focus subsequent studies primarily on this prosurvival response since it was observed with both primary rodent cortical neurons and human neuronal cells derived from an immortalized cell line. Furthermore, the ability of CNS neurons to survive viral infection, even in the absence of complete pathogen clearance, may represent an important component of the physiological response of these vital cells to infection with neurotropic viruses.

IRF-3 mediates a neuronal cytoprotective response against neurotropic flavivirus but not bunyavirus infection. We evaluated whether the IRF-3-dependent cytoprotective response of cultured neurons was restricted to alphaviruses or extended to other neurotropic viruses. For these experiments we used LACV, a bunyavirus that is the most common cause of pediatric arboviral encephalitis in the United States (41), and SLEV, a neurotropic flavivirus responsible for both endemic and epidemic cases of arboviral encephalitis in the United States (42). We initially examined the IFN-β transcriptional response to LACV or SLEV infection in BE(2)-C/m cells by semiquantitative RT-PCR (Fig. 5A). In

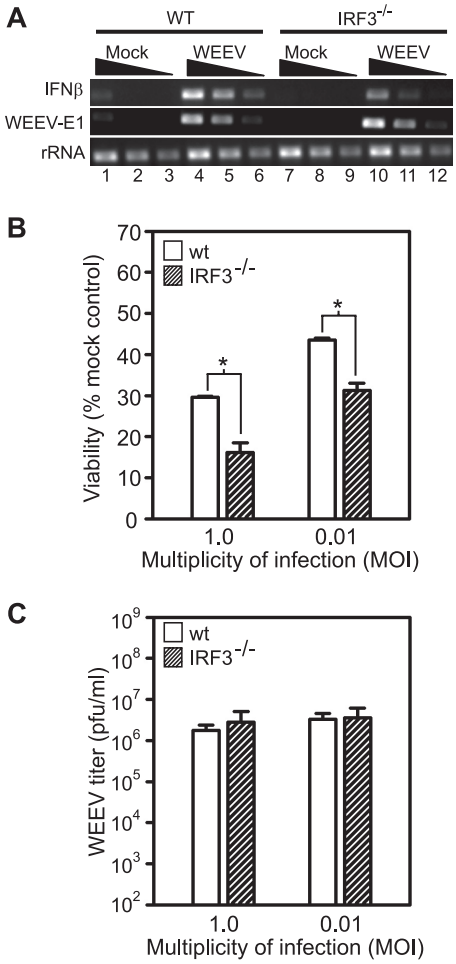

FIG 4 IRF-3 mediates IFN-β transcriptional induction and enhances neuronal survival in primary mouse cortical neurons. (A) Primary cortical neurons derived from wild-type (wt) C57BL/6 (lanes 1 to 6) and IRF-3$^{-/-}$ (lanes 7 to 12) mice were either mock infected (lanes 1 to 3 and 7 to 9) or infected with WEEV at an MOI of 1 (lanes 4 to 6 and 10 to 12), and IFN-β, WEEV E1, and rRNA transcript levels were assayed by semiquantitative RT-PCR at 20 hpi. Adjacent lanes for individual samples represent results using 10-fold dilutions of cDNA. (B and C) Primary cortical neurons derived from wt C57BL/6 or IRF-3$^{-/-}$ mice were infected with WEEV at the indicated MOI, and the percentages of viability relative to mock-infected controls (B) and infectious viral titers in supernatants (C) were measured at 48 hpi. Viral titers also were measured at 8 and 20 hpi and showed no difference between wt and IRF-3$^{-/-}$ neurons for an MOI of either 1 or 0.01 (data not shown). *, $P < 0.05$.

control cells transfected with empty vector, both viruses induced IFN-β mRNA transcription, although the level of induction was lower in response to infection with LACV (Fig. 5A, lanes 4 to 6) compared to that with SLEV (Fig. 5A, lanes 7 to 9). Disruption of IRF-3 function via expression of dnIRF-3 inhibited SLEV-induced IFN-β mRNA accumulation by ~10-fold (Fig. 5A, lanes 16 to 18), whereas a less prominent reduction was observed in LACV-induced IFN-β mRNA accumulation (Fig. 5A, lanes 13 to 15). We also examined the impact of dnIRF-3 expression on virus-induced CPE and found similar differential effects. Neuronal cells expressing dnIRF-3 were significantly more susceptible to SLEV-mediated CPE (Fig. 5B) but not to LACV-mediated CPE (Fig. 5C), regardless of viral inoculum. These results suggested that IRF-3

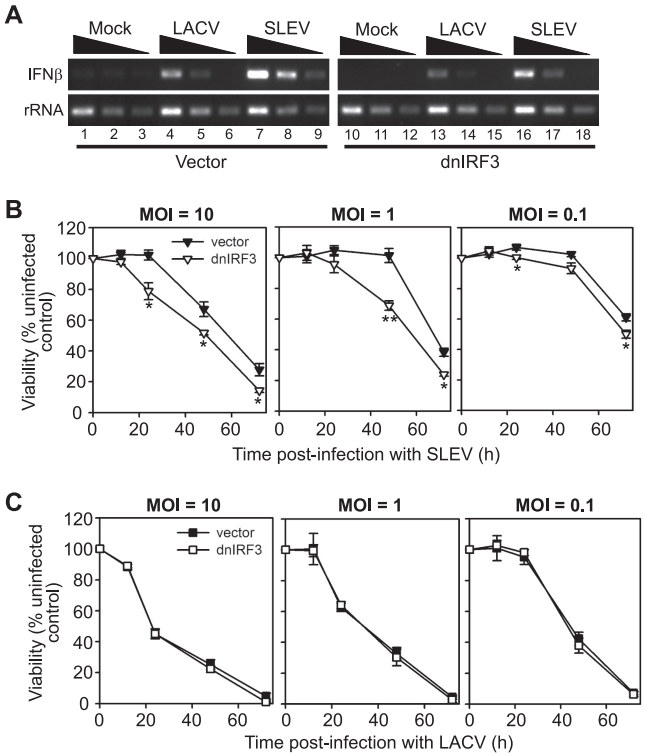

FIG 5 IRF-3 mediates IFN-β transcriptional induction and enhances neuronal survival in BE(2)-C/m cells in response to SLEV but not LACV infection. (A) BE(2)-C/m cells stably transfected with empty vector (lanes 1 to 9) or a constitutively active dnIRF-3 expression plasmid (lanes 10 to 18) were mock infected (lanes 1 to 3 and 10 to 12) or infected with LACV (lanes 4 to 6 and 13 to 15) or SLEV at an MOI of 1 (lanes 7–9 and 16–18), and IFN-β and rRNA transcript levels were assayed by semiquantitative RT-PCR at 20 hpi. Adjacent lanes for individual samples represent results using 10-fold dilutions of cDNA. (B and C) BE(2)-C/m cells stably transfected with empty control vector (closed symbols) or a dnIRF-3 construct (open symbols) were infected with SLEV (B) or LACV (C) at the indicated MOI, and viability relative to mock-infected controls was measured from 12 to 72 hpi. *, $P < 0.05$; **, $P < 0.005$ (compared to virus-infected cells expressing control vector at the corresponding time point).

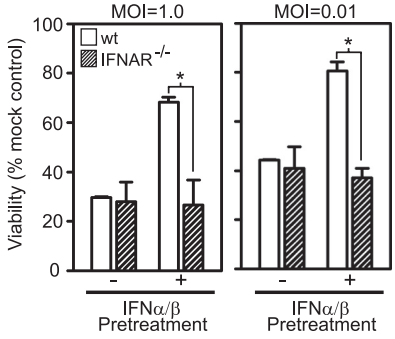

FIG 6 Neuronal prosurvival responses to WEEV are independent of type I IFN autocrine or paracrine activity. Cortical neurons from wt C57BL/6 or IFNAR$^{-/-}$ mice were mock treated or stimulated with 100 U/ml of mouse IFN-α/β for 24 h and infected with WEEV at the indicated MOI, and cell viability relative to mock-infected controls was assessed 48 hpi. *, $P \leq 0.05$.

was important for the neuronal cytoprotective response to some, but not all, neurotropic arboviruses.

Neuronal IRF-3-dependent cytoprotective response is independent of type I IFN autocrine or paracrine signaling. The observation that a dnIRF-3 mutant lacking a DNA binding domain enhanced WEEV-mediated CPE in BE(2)-C/m neuronal cells suggested that IRF-3-dependent transcriptional activity was involved in the cytoprotective response. One explanation for this observation is that WEEV might induce type I IFN production and secretion in BE(2)-C/m cells, thereby initiating an autocrine or paracrine antiviral and prosurvival pathway. Although WEEV infection induced IFN-β transcription in BE(2)-C/m cells (Fig. 1), and these cells are capable of synthesizing and secreting IFN-β in response to artificial PRR ligands (24), we have previously shown that neutralizing antibodies against type I IFNs do not impact WEEV-induced CPE (34). Furthermore, WEEV infection did not activate an IFN-β-dependent ISRE reporter, and we have not detected any measurable secreted type I IFNs in supernatants of infected neuronal cells (data not shown). To provide definitive genetic validation of these results, we prepared primary cortical neuron cultures from mice lacking the type I IFN receptor (IFNAR$^{-/-}$) and control mice. Whereas control cultures pretreated with type I IFNs showed the expected protective effects in neurons derived from wild-type mice, there were no differences in WEEV-induced CPE between untreated neurons isolated from wild-type and IFNAR$^{-/-}$ mice irrespective of virus inoculum (Fig. 6). Taken together, these data indicated that the IRF-3-dependent neuronal cytoprotective response to WEEV infection was independent of autocrine or paracrine type I IFN signaling.

WEEV infection inhibits poly(I-C)-induced activation of PRR pathways in neurons. PRR pathway activation in neurons can occur rapidly after PAMP ligand-receptor interaction, as we have previously observed IFN-β mRNA induction within 5 h of poly(I-C) stimulation (24). Although we observed IFN-β mRNA induction after WEEV infection (Fig. 1), we noted in initial time course experiments a delay of 10 h or more between WEEV infection and IFN-β gene induction (data not shown), despite readily detected virus replication by 6 hpi (34). This suggested that WEEV might actively antagonize PRR pathway signaling, similar to several other viruses (14, 43, 44). To test this hypothesis, we examined the impact of WEEV infection on poly(I-C)-induced gene activation in BE(2)-C/m cells (Fig. 7). We measured the activation of either ISRE promoter-driven (Fig. 7A) or NF-κB promoter-driven (Fig. 7B) reporter genes, used either extracellular or transfected poly(I-C) to stimulate surface or cytosolic PRRs, respectively, and altered the sequence of WEEV infection and artificial ligand stimulation. We also assessed cell viability to account for possible virus-induced CPE, although there is typically only mild cell death at the 16-to-20-hpi time point used for analysis in these assays (34). WEEV infection at an MOI of 1 suppressed both extracellular and transfected poly(I-C)-induced ISRE activation in BE(2)-C/m cells, and the level of suppression was increased if cells were infected 1.5 h prior to poly(I-C) stimulation (Fig. 7A, left graph) in comparison to infection 3 h after stimulation (Fig. 7A, right graph). This suppression was likely due to disruption of poly(I-C)-stimulated IFN-β induction, as WEEV infection did not suppress exogenous type I IFN-mediated ISRE activation. Similar results were obtained with the NF-κB reporter-expressing cells (Fig. 7B), although virus infection also suppressed TNF-α-stimulated reporter gene activation, suggesting that WEEV may inhibit multiple signaling pathways or a component shared be-

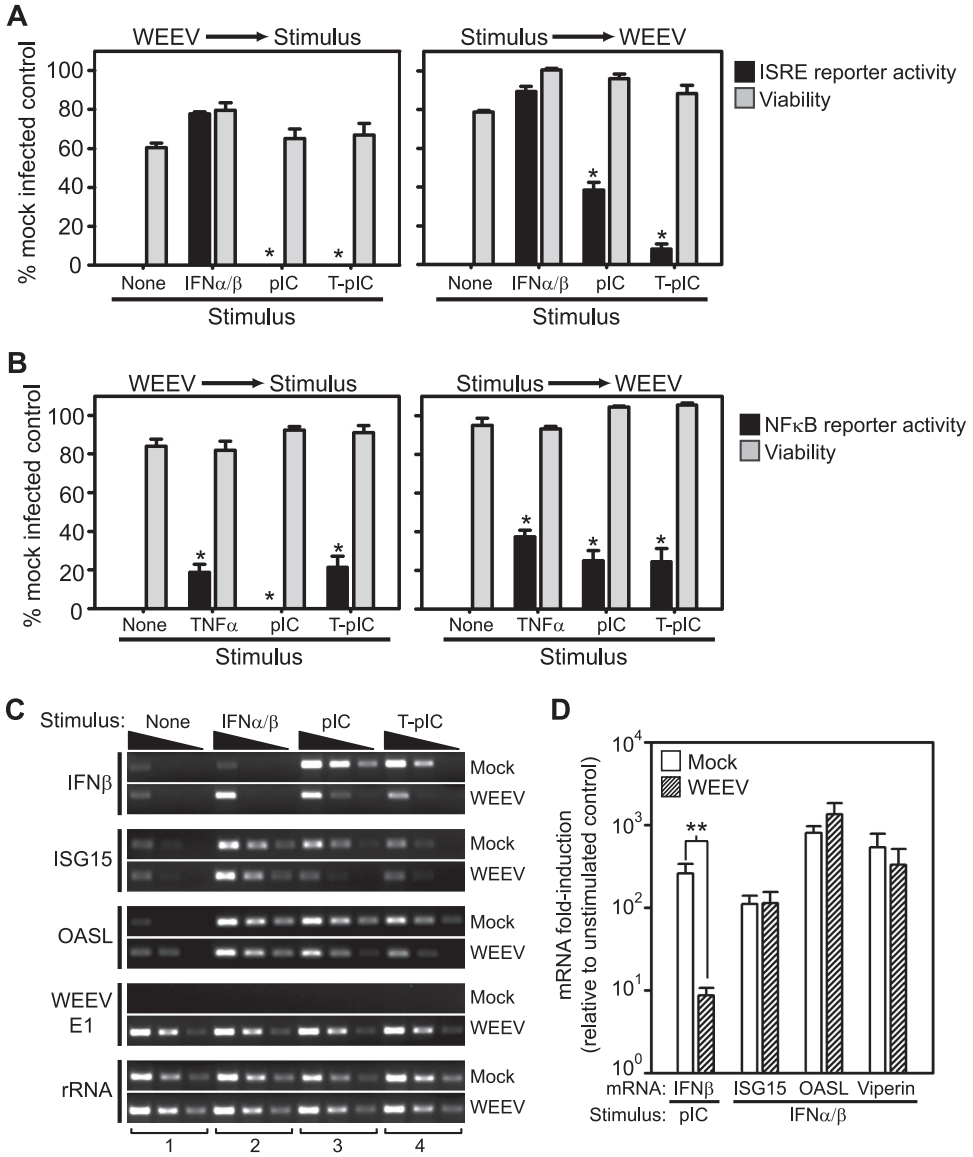

FIG 7 WEEV infection inhibits neuronal PRR pathway activity. (A) BE(2)-C/m ISRE promoter-reporter cells were infected with WEEV at an MOI of 1 for 1.5 h and subsequently treated with the indicated stimulus (left graph) or pretreated with the indicated stimulus for 3 h prior to infection with WEEV (right graph), and both reporter activity and viability were assessed relative to mock-infected controls at 16 to 20 hpi. We used 100 U/ml IFN-α/β-A/D, 50 μg/ml extracellular poly(I-C) (pIC), and 500 ng/ml transfected poly(I-C) (T-pIC) for stimulation. *, $P \leq 0.05$ compared to appropriate mock-infected control. (B) BE(2)-C/m NF-κB promoter-reporter cells were treated and analyzed as described above for panel A except that 25 ng/ml TNF-α was used instead of IFN-α/β-A/D. (C) BE(2)-C/m cells were mock infected (upper gel in each gene-specific group) or infected with WEEV at an MOI of 1 for 3 h (lower gel in each gene-specific group) and treated with the indicated stimulus, and transcripts for the indicated genes were analyzed by semiquantitative RT-PCR 4 h after stimulation. Adjacent lanes for individual samples represent results using 10-fold dilutions of cDNA. (D) BE(2)-C/m cells were infected and stimulated as described in panel B except that WEEV was used at an MOI of 10 and gene transcripts were analyzed by qRT-PCR 4 h after stimulation. **, $P < 0.0001$.

tween TNF-α receptor and PRR pathways but not present in the IFNAR signaling pathway.

We also assessed WEEV-mediated inhibition of PRR pathway activation by directly examining IFN-β mRNA induction by semiquantitative RT-PCR after extracellular and transfected poly(I-C) stimulation (Fig. 7C). As a control, we measured mRNA production of the IFN-stimulated genes ISG15 and OASL, which are induced by both IRF-3-dependent PRR signaling and IFNAR signaling (45). Consistent with the reporter gene experiments described above, at an MOI of 1 WEEV infection 3 h prior to ligand stimulation suppressed poly(I-C)-induced IFN-β, ISG15, and OASL mRNA upregulation (Fig. 7C, group 3) but not exogenous type I IFN-induced ISG15 or OASL mRNA upregulation (Fig. 7C, group 2). Similar results were obtained with additional IFN-stimulated genes, including MxB and Rsad2/viperin (data not shown). We further analyzed and quantitated the impact of WEEV infection on poly(I-C)- and type I IFN-induced gene transcription by qRT-PCR (Fig. 7D). For these experiments we also used an MOI of 10 to ensure that the majority of cells were infected (Fig. 3B). WEEV infection reduced poly(I-C)-induced IFN-β mRNA upregulation by >95% but had no significant effect on type I IFN-induced ISG15, OASL, or viperin mRNA upregulation (Fig. 7D). We con-

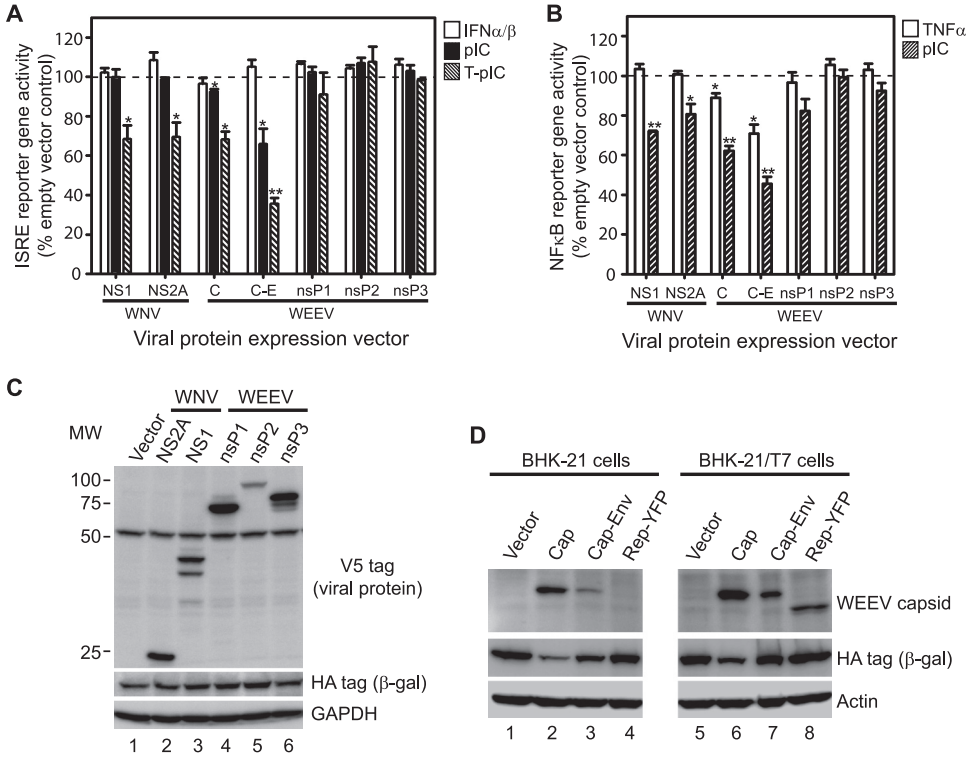

FIG 8 WEEV structural proteins inhibit PRR signaling in neuronal cells. (A) BE(2)-C/m ISRE promoter-reporter cells were cotransfected with a control HA-tagged β-galactosidase (β-gal) expression vector and a second vector encoding the indicated WNV (NS1, NS2A) or WEEV (capsid [C], capsid-envelope [C-E], nsP1, nsP2, or nsP3) genes. Cells were subsequently stimulated 48 h after transfection with 100 U/ml IFN-α-A/D, 50 μg/ml extracellular poly(I-C) (pIC), or 700 ng/ml transfected poly(I-C) (T-pIC), and reporter gene activity was measured 24 h after stimulation. Results are expressed relative to cells cotransfected with empty vector (dashed line). We observed no significant cytotoxicity from transient overexpression of any viral gene, as assessed by MTT assay (data not shown). *, $P < 0.05$; **, $P < 0.005$. (B) BE(2)-C/m NF-κB promoter-reporter cells were transfected and stimulated as described above for panel A except that 25 ng/ml TNF-α was used instead of IFN-α-A/D. (C) Lysates from BE(2)-C/m cells transfected with WNV (lanes 2 and 3) or WEEV (lanes 4 to 6) nonstructural protein expression vectors as described for panels A and B were analyzed by immunoblotting for HA-tagged β-gal, V5-tagged viral proteins, and GAPDH as a loading control. Note the cross-reactivity of the V5 antibody with an ~50-kDa protein in all samples. MW, molecular weight (in thousands). (D) Lysates from BHK-21 cells (left blots) or BHK-21 cells stably expressing bacteriophage T7 RNA polymerase (BHK-21/T7; right blots) cotransfected with a control HA-tagged β-gal expression vector and a second vector encoding WEEV capsid (Cap; lanes 2 and 6), capsid-envelope (Cap-Env; lanes 3 and 7), or T7 promoter-driven capsid/YFP chimera WEEV replicon (Rep-YFP; lanes 4 and 8) were analyzed by immunoblotting for WEEV capsid, HA-tagged β-gal, and actin as a loading control.

cluded from these results that WEEV infection suppressed PRR-mediated signal transduction in BE(2)-C/m neuronal cells without globally inhibiting cell signaling pathways.

WEEV capsid protein suppresses PRR pathways. Alphaviruses encode seven major proteins: three structural proteins, including the capsid and two envelope glycoproteins designated E1 and E2, and four nonstructural proteins designated nsP1 through nsP4 (46). To determine which viral protein(s) contributed to WEEV-mediated suppression of PRR pathway signaling, we cloned the entire structural region (C-E) and individual capsid (C), nsP1, nsP2, and nsP3 genes into cytomegalovirus (CMV) promoter-driven plasmids for transient expression in mammalian cells. Of note, we were unable to express full-length WEEV nsP4 as an isolated protein, possibly because of its short half-life and relative instability in cells (46). We subsequently transiently transfected these viral genes into BE(2)-C/m cell lines expressing ISRE- and NF-κB-promoter reporter genes and measured reporter gene activity after poly(I-C) or control stimulation (Fig. 8). As controls, we cloned and expressed the WNV NS1 and NS2A proteins, which have previously been shown to suppress PRR pathway activation (47, 48).

Ectopic expression of WEEV capsid and complete structural genes suppressed transfected poly(I-C)-induced ISRE reporter gene activation, whereas expression of WEEV nsP1, nsP2, or nsP3 had no effect (Fig. 8A). Although the magnitude of suppression was only 30 to 50%, it was consistent with that seen with the positive controls WNV NS1 and NS2A. Expression of the entire WEEV structural genes, and to a lesser extent the individual capsid gene, also suppressed extracellular poly(I-C)-induced responses, whereas no suppression with this ligand was seen with WNV NS1 or NS2A or any of the WEEV nonstructural proteins. None of the constructs suppressed exogenous type I IFN-induced ISRE activation, consistent with the infection experiments described above (Fig. 7). We conducted similar experiments using BE(2)-C/m cells that contained an NF-κB promoter-driven reporter gene, and we found that ectopic expression of WEEV capsid or the complete structural gene cassette, as well as the controls WNV NS1 and NS2A, suppressed extracellular poly(I-C)-induced reporter gene activation, whereas WEEV nsP1, nsP2, and nsP3 had no significant effect (Fig. 8B). In contrast to the ISRE-reporter gene experiments, ectopic expression of WEEV capsid or complete structural genes also suppressed TNF-α-induced NF-κB-reporter gene activation, which was consistent with infection experiments (Fig. 7B).

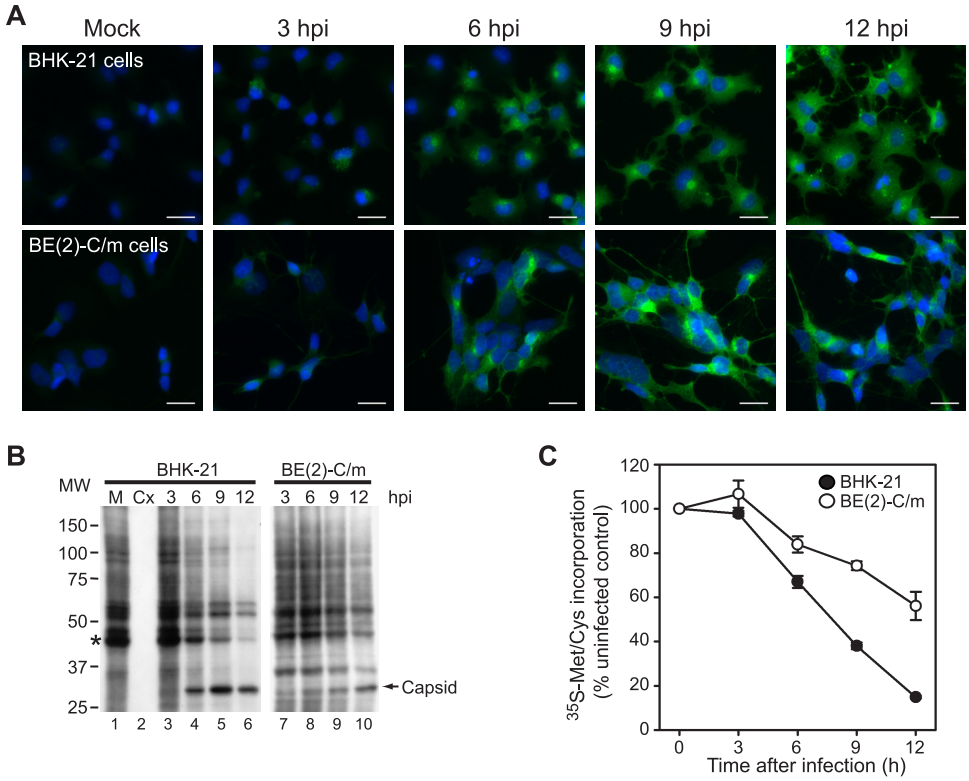

FIG 9 WEEV-mediated suppression of host translation is reduced in neuronal cells. (A) Control BHK-21 (upper images) or BE(2)-C/m (lower images) were infected with WEEV at an MOI of 10 and analyzed by immunofluorescence microscopy at the indicated times postinfection. Representative overlaid images from one of two independent experiments are shown, where blue indicates DAPI-stained nuclei and green indicates WEEV-infected cells. Scale bars, 25 μm. (B) Control BHK-21 (lanes 1 to 6) or BE(2)-C/m (lanes 7 to 10) were infected with WEEV at an MOI of 10 and labeled with 50 μCi/ml [^{35}S]methionine-cysteine for 30 min prior to harvesting at 3, 6, 9, and 12 hpi, and lysates were analyzed by SDS-PAGE and fluorography. Mock-infected (lane 1) and cycloheximide-treated (lane 2) BHK-21 cells are shown as representative controls. Molecular weight (MW) markers (in thousands) are shown on the left, and presumptive WEEV capsid protein is indicated by the arrow. (C) Translation of the cellular protein at ~45 kDa, marked by the asterisk in panel B, was quantitated by densitometry for BHK-21 and BE(2)-C/m cells, and results are expressed as the percentage of uninfected control cells.

It was unclear why WNV NS1 and NS2A, in contrast to WEEV structural genes, showed differential suppressive effects on ISRE promoter activity between extracellular and transfected poly(I-C) delivery (Fig. 8A), whereas proteins from both viruses suppressed extracellular poly(I-C)-induced NF-κB activation (Fig. 8B). Possibly, the mechanisms by which WNV NS1 or NS2A and WEEV capsid suppress PRR-mediated innate immune pathways are different.

To confirm these findings, we verified protein expression by immunoblotting for the C-terminal V5 epitope tag that was used in the plasmid design. We established that WNV NS1 and NS2A and WEEV nsP1, nsP2, and nsP3 were all expressed in transiently transfected BE(2)-C/m cells and that expression levels did not correlate with suppression of poly(I-C)-induced responses (Fig. 8C). The WEEV capsid and complete structural protein expression constructs did not contain a V5 epitope tag, and we were unable to detect native capsid or envelope proteins using commercially available antibodies against WEEV, although RT-PCR readily demonstrated mRNA production (data not shown). The inability to detect capsid protein by immunoblotting was likely due to low-level expression in BE(2)-C/m cells, as we routinely obtained 60 to 70% transfection efficiency with BE(2)-C/m cells and we could readily detect capsid protein using the same reagents in lysates from BHK-21 cells transiently transfected with the individual WEEV capsid protein (Fig. 8D, lane 2) or the entire WEEV structural region (Fig. 8D, lane 3). To validate the specificity of WEEV capsid immunoblotting, we used lysates from cells transfected with a plasmid encoding a T7 promoter-driven WEEV replicon that produces a chimeric and truncated capsid-YFP protein during active viral RNA replication (33). As expected, this truncated capsid was detected with the anti-capsid antibodies only in BHK-21 cells that expressed bacteriophage T7 RNA polymerase (Fig. 8D, compare lanes 4 and 8). Combined with the reporter gene experiments described above, these results suggested that WEEV capsid protein inhibited PRR-mediated signaling pathways in human neuronal cells.

One potential confounding factor with the viral protein expression studies is that the capsid proteins of the related neurotropic alphaviruses VEEV and EEEV suppress host gene transcription and translation (49–51). However, WEEV capsid protein did not globally inhibit host signal transduction and gene expression as measured by transcription and reporter gene assays (Fig. 7). Nevertheless, to directly assess the impact of WEEV infection on host gene expression, we examined the kinetics of virus-mediated host translational suppression using metabolic labeling with [^{35}S]methionine-cysteine in cells infected with WEEV at an MOI of 10 (Fig. 9). As a control, we used BHK-21 cells, which show prominent New and Old World alphavirus-mediated inhi-

bition of host translation (51, 52). Immunofluorescence microscopy showed no qualitative differences in the temporal appearance of WEEV antigen-positive cells between BHK-21 and BE(2)-C/m cells (Fig. 9A), suggesting similar initial permissiveness to a high MOI inoculum. As expected, WEEV infection rapidly suppressed host translation in BHK-21 cells, as cellular protein synthesis was reduced by >80% at 12 hpi (Fig. 9C, closed symbols) and viral capsid protein synthesis was readily apparent (Fig. 9B, lanes 3 to 6). In contrast, translation in BE(2)-C/m cells was less susceptible to WEEV inhibition, as cellular protein synthesis was suppressed by ~40% at 12 hpi (Fig. 9C, open symbols) and accumulation of viral capsid protein was less prominent (Fig. 9B, lanes 7 to 10). More importantly, WEEV infection suppressed cellular translation in BE(2)-C/m cells by only 15 to 25% at 6 to 9 hpi (Fig. 9C), whereas it potently suppressed antiviral PRR signaling at 7 hpi (Fig. 7D). Thus, WEEV-mediated host translational inhibition was delayed compared to PRR pathway inhibition and unlikely to explain the suppressive effects of WEEV capsid on innate immune system activation.

WEEV capsid protein inhibits antiviral PRR signaling downstream of IRF-3 activation in neurons. Viruses antagonize innate immune responses through several different mechanisms, including sequestration or degradation of PRRs or signal transduction components and shielding viral PAMPs from detection (43, 44). To examine the mechanism(s) by which WEEV capsid protein inhibits antiviral PRR signaling in neurons, we conducted epistasis experiments to assess the level at which suppression occurred (Fig. 10). To initiate signaling at discrete levels within the PRR pathway we transfected ISRE reporter-bearing BE(2)-C/m cells with vectors expressing a constitutively active TLR adapter molecule, TRIF (saTRIF), the cytosolic PRR MDA5, or a constitutively active downstream transcription factor, IRF-3 (saIRF-3). These vectors were cotransfected with either an empty vector control, dnIRF-3 control, or expression vectors encoding WEEV nsP1, capsid, or complete structural genes, and PRR pathway activation was measured as autocrine or paracrine type I IFN-mediated ISRE activity (Fig. 10A). Ectopic expression of dnIRF-3 suppressed ISRE reporter gene activity stimulated by adapter protein saTRIF and the PRR MDA5 but had no effect on reporter activity stimulated by saIRF-3, confirming that this constitutively active transcription factor did not require upstream PRR pathway signals for activation. In contrast, WEEV capsid and structural gene expression inhibited saTRIF-, MDA5-, and saIRF-3-mediated activation of ISRE reporter gene activation, whereas WEEV nsP1 expression had no effect in these assays, consistent with poly(I-C)-induced responses (Fig. 8A).

The ability of WEEV to inhibit host protein expression (Fig. 9), possibly via capsid-mediated suppression similar to that of VEEV and EEEV (49–51), represented a potential confounding factor in the epistasis experiments. To examine the impact of WEEV capsid on host-dependent expression of plasmid-encoded PRR components, we performed immunoblotting experiments (Fig. 10B). Expression of WEEV capsid and the entire structural region reduced vector-mediated saTRIF, MDA5, and saIRF-3 expression to various levels, but this suppression did not correlate with the level of ISRE reporter gene suppression. For example, transfection of WEEV capsid gene reduced exogenous saTRIF, MDA5, and saIRF-3 levels by ~80%, 50%, and 10%, respectively (Fig. 10B, lanes 8 to 10, compared to control lanes 2 to 4), but reduced ISRE reporter gene activity by ~80% for all three samples (Fig. 10A).

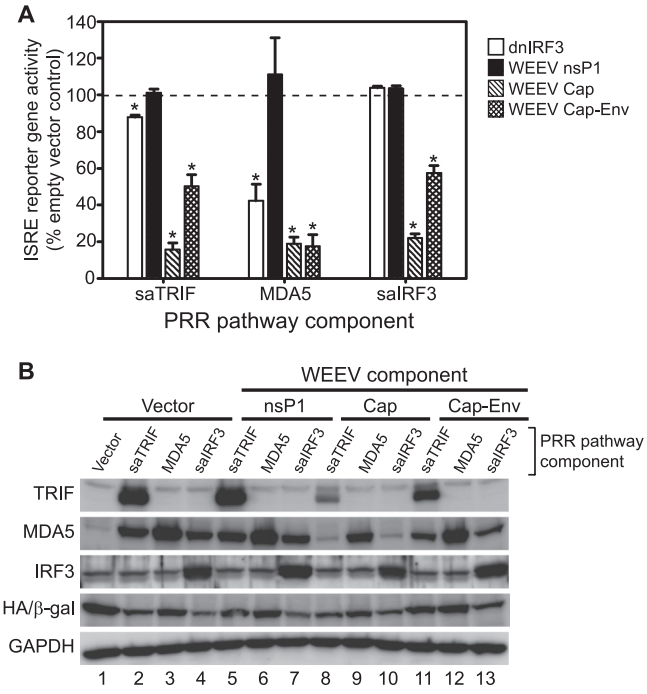

FIG 10 WEEV structural proteins inhibit neuronal antiviral PRR signaling in neurons at a step downstream of IRF-3 activation. (A) BE(2)-C/m ISRE promoter-reporter cells were cotransfected with a control HA-tagged β-galactosidase (β-gal) expression vector, a second vector containing no insert (empty vector control) or encoding a dominant negative IRF-3 (dnIRF-3) or the WEEV nsP1, capsid (Cap), or capsid-envelope (Cap-Env) protein, and a third vector encoding the indicated superactive (sa) or wild-type PRR-pathway component. Reporter gene activity was measured 48 h after transfection, and results are expressed relative to empty vector transfected controls (dashed line). *, $P \leq 0.05$. (B) Lysates from the transfected cells described in panel A were analyzed by immunoblotting for TRIF, MDA5, IRF-3, HA-tagged β-gal, and GAPDH as a loading control.

Results with the WEEV structural gene cassette showed a similar lack of correlation, where exogenous saTRIF, MDA5, and saIRF-3 levels were reduced by ~45%, 5%, and <1%, respectively (Fig. 10B, lanes 11 to 13 compared to control lanes 2 to 4), but reduced ISRE reporter gene activity by ~50%, 80%, and 40% for the corresponding samples (Fig. 10A). Taken together, these results suggested that WEEV capsid protein suppressed PRR pathway signaling downstream of IRF-3 activation and that this inhibitory activity was independent of global suppression of host gene and protein expression.

DISCUSSION

In this report we examined the functional impact of IRF-3-dependent innate immune pathways in neuronal cells infected with globally relevant arboviruses. We drew five main conclusions from these studies. First, WEEV activated neuronal PRR pathways in a replication- and IRF-3-dependent manner. Second, IRF-3 mediated a neuronal cytoprotective response that was active against some (e.g., WEEV and SLEV) but not all neurotropic arboviruses. Third, IRF-3-dependent cytoprotective responses in neurons were largely independent of autocrine or paracrine type I IFN activity. Fourth, WEEV potently inhibited innate immune signaling in neurons. Fifth, the inhibition of innate immune signaling was mediated by WEEV capsid, which suppressed signal transduc-

tion downstream of IRF-3 activation and appeared to be independent of capsid-mediated inhibition of host macromolecular synthesis. These results highlight the interplay between the neuronal innate immune response and neurotropic arboviruses and identify a novel IRF-3-dependent cytoprotective response in neurons.

Innate immune responses mediated by the transcription factor IRF-3 have multiple functions in the control of viral infections. One example is the suppression of viral replication through the activation of antiviral genes such as PKR, OAS, or Rsad2/viperin, either through direct transcriptional regulation or indirectly via induction of type I IFNs (53–55). Although we observed an IRF-3-dependent decrease in virion production with WEEV-infected BE(2)-C/m human neuronal cells, we saw no impact of IRF-3 on virus production in primary mouse cortical neurons. This may represent a species-specific difference or, alternatively, a disparity between primary and immortalized cells. Regardless, in both types of neurons we saw consistent IRF-3-dependent cytoprotective effects after WEEV infection irrespective of viral inoculum. However, this effect was not universal for all arboviruses tested, as IRF-3 also protected against SLEV- but not LACV-mediated CPE, suggesting that complex and poorly defined interactions between virus and host cells ultimately control the neuronal response to infection. An IRF-3-dependent prosurvival activity in neurons has potential physiologic importance, as mature CNS neurons are largely irreplaceable. Thus, an innate immune response in neurons may require a balance between promoting cell survival and limiting virus replication, albeit incompletely. Such a balanced response may not be necessary for cells that can be readily replaced, as rapid cell death may be a primary mechanism to prevent virus spread. Indeed, IRF-3-dependent proapoptotic responses in nonneuronal cells have been described after infection with several RNA and DNA viruses (56–59).

The mechanism(s) whereby an IRF-3-mediated type I IFN-independent response triggered by WEEV or SLEV infection promotes neuronal survival is unknown. IRF-3 modulates the expression of a wide variety of cellular genes in addition to type I IFNs (45), and preliminary studies have identified several candidate IRF-3-dependent genes induced by WEEV infection that have been associated with resistance to neurotropic arbovirus-mediated CPE, including MxA and OASL (D. Peltier, J. Farmer, and D. Miller, unpublished data). An alternative candidate is IFIT1, which was recently shown to affect neuronal survival after WNV infection (60) and can also suppress alphavirus replication (55). Innate immune responses triggered by PRR ligation often involve multiple and complex overlapping pathways that control hundreds of genes (11), and therefore the result of enhanced cell survival is unlikely to be due to a single or even small subset of cellular genes. An additional signaling pathway that has previously been associated with enhanced cell survival after virus infection is NF-κB activation, which induces protective antiapoptotic activity in many cell types (61) and may mediate neurogenesis (62) and protection of neurons from ischemia (63, 64). We have previously demonstrated that differentiated BE(2)-C/m human neuronal cells activate NF-κB in response to poly(I-C) or SeV stimulation (24). Studies are in progress to further define the roles of NF-κB-mediated responses and their interactions with IRF-3-mediated responses in promoting neuronal survival after infection with WEEV and other neurotropic arboviruses.

The observation that replication-competent WEEV was necessary to induce IRF-3-mediated responses suggested that viral RNA replication in the cytoplasm was an important trigger of PRR activation in neuronal cells. Human neurons possess functional TLR3, MDA5, and RIG-I receptors (19–25), although the receptors responsible for the IRF-3-dependent responses we observed are currently unknown. There are limited published studies of PRR activation by New World alphaviruses (e.g., WEEV, EEEV, or VEEV), although Old World alphaviruses (e.g., chikungunya or Sindbis viruses) can activate MDA5 or RIG-I and require the PRR adapter IPS-I (65–68). Studies with WNV suggest that multiple PRRs contribute to activating cell-intrinsic host defense responses to neurotropic arboviruses, potentially in a cell type-specific manner (3–6, 29). Preliminary studies suggest that both MDA5 and RIG-I contribute to neuronal innate immune responses after WEEV infection in cultured cells (D. Peltier and D. Miller, unpublished data), but definitive results to implicate specific PRR pathways after infection with WEEV or other neurotropic arboviruses await detailed *in vivo* studies with neuron-specific conditional knockout mice.

Most successful viruses possess targeted or global countermeasures to prevent innate immune pathway activation that allow them to efficiently replicate, avoid detection, and disseminate (14, 43, 44). A strategy of host transcriptional or translational shutoff is employed by several viruses and includes the activity of the NSs protein of bunyaviruses (69) and the nsP2 protein of Old World alphaviruses (51). The New World encephalitic alphaviruses VEEV and EEEV also globally suppress host RNA transcription and translation, although this effect is mediated by the capsid protein rather than nsP2 (49–51) and may involve disruption of nuclear translocation (70, 71). We also mapped the viral antagonism of IRF-3 to the capsid protein of WEEV, although our ectopic expression experiments do not fully exclude a potential contributory role of viral nonstructural proteins in IRF-3 antagonism in the context of replication-competent virus. In addition, our results differed somewhat from published studies with other alphaviruses, as we observed no significant suppression of type I IFN-mediated ISG induction with WEEV infection, even under high-inoculum conditions where virtually all cells were infected. In contrast, VEE, Sindbis, and chikungunya viruses all suppress the type I IFN-Jak-STAT pathway (72–75). These discrepancies may reflect true biological differences between viral countermeasures of New and Old World alphaviruses, at least for Sindbis and chikungunya virus, or may be due in part to methodological differences, such as the use of replicons (73, 75) or nonneuronal cells (72–74), whereas we focused primarily on neuronal cells, replication-competent infectious virus, and exogenous plasmid-directed expression of specific viral proteins. However, direct comparison with one published study can be made that suggests potential intrinsic differences between WEEV and VEEV. Yin et al. showed that VEEV infection of primary mouse cortical neurons potently inhibited IFN-α/β-induced ISG upregulation, which was attributed to VEEV structural proteins as GFP-expressing replicons did not display similar inhibitory activity (75). We did not examine the effect of WEEV infection or exogenous capsid expression on individual steps in the type IFN signaling pathway, and thus we cannot exclude a direct impact of WEEV on specific signaling events such as STAT1/2 phosphorylation or nuclear translocation, as demonstrated for VEEV (75). However, our results suggest that any such inhibitory activity, even if present, had negligible functional impact on ISG induction in cultured neuronal cells. One

intriguing yet speculative hypothesis is that WEEV capsid disrupts nuclear translocation of activated IRF-3, in a manner analogous to the proposed mechanism by which VEEV capsid protein suppresses host gene expression (70, 71), albeit with potentially more nuclear transport selectivity. Detailed studies to examine the underlying mechanism(s) responsible for WEEV capsid-mediated suppression of innate immune responses are currently in progress to directly test this hypothesis.

In summary, we have identified a cell-intrinsic innate immune response mediated by IRF-3 that promotes cell survival in neurons infected with WEEV as well as another neurotropic arbovirus, SLEV. The conclusions that WEEV both induces and suppresses IRF-3-dependent responses in neurons appear contradictory, but they may simply represent the ongoing struggle between cellular innate immune responses and virus-directed countermeasures. Although WEEV replication induced IRF-3-dependent responses, IFN-β mRNA induction in infected neurons was delayed in comparison to poly(I-C)-stimulated responses. Furthermore, neuronal cytoprotective responses eventually failed, even with low MOI inocula and in IRF-3-competent cells, suggesting that WEEV-directed countermeasures are sufficient to overcome neuronal innate immune responses, at least within isolated *in vitro* experimental conditions. Our studies suggest that therapeutics designed to modulate IRF-3 function or directly target viral countermeasures may augment cytoprotective responses, prolong neuronal survival, and potentially allow the full activation of virus-clearing adaptive immune responses (12).

ACKNOWLEDGMENTS

We thank Sue O'Shea, Richard Kinney, Marc Hershenson, Robert Tesh, and Valery Grdzelishvili for providing reagents and technical assistance. We thank all members of the Miller lab for their helpful comments on the research and manuscript.

This work was funded by the National Institute of Allergy and Infectious Diseases grants U54 AI057153 (Region V Great Lakes Regional Center of Excellence for Biodefense and Emerging Infectious Diseases Research Career Development Award to D.J.M.), R21 A1076975 (to D.J.M.), T32 A1007528 (to D.C.P.), U19 AI083019 (to M.S.D. and H.M.L.), National Institute of General Medical Sciences grant T32 GM007863 (to D.C.P. and J.R.F.), and National Institute of Neurological Disorders and Stroke grant F30 NS065566 (to J.R.F.).

REFERENCES

1. **Gubler DJ.** 2002. The global emergence/resurgence of arboviral diseases as public health problems. Arch. Med. Res. **33**:330–342.
2. **Sidwell RW, Smee DF.** 2003. Viruses of the *Bunya-* and *Togaviridae* families: potential as bioterrorism agents and means of control. Antiviral Res. **57**:101–111.
3. **Daffis S, Samuel MA, Keller BC, Gale M, Diamond MS.** 2007. Cell-specific IRF-3 responses protect against West Nile virus infection by interferon-dependent and -independent mechanisms. PLoS Pathog. **3**:e106. doi:10.1371/journal.ppat.0030106.
4. **Daffis S, Samuel MA, Suthar MS, Gale M, Jr, Diamond MS.** 2008. Toll-like receptor 3 has a protective role against West Nile virus infection. J. Virol. **82**:10349–10358.
5. **Daffis S, Samuel MA, Suthar MS, Keller BC, Gale M, Jr, Diamond MS.** 2008. Interferon regulatory factor IRF-7 induces the antiviral α interferon response and protects against lethal West Nile virus infection. J. Virol. **82**:8465–8475.
6. **Daffis S, Suthar MS, Szretter KJ, Gale M, Jr, Diamond MS.** 2009. Induction of IFN-β and the innate antiviral response in myeloid cells occurs through an IPS-1-dependent signal that does not require IRF-3 and IRF-7. PLoS Pathog. **5**:e1000607. doi:10.1371/journal.ppat.1000607.
7. **Detje CN, Meyer T, Schmidt H, Kreuz D, Rose JK, Bechmann I, Prinz M, Kalinke U.** 2009. Local type I IFN receptor signaling protects against virus spread within the central nervous system. J. Immunol. **182**:2297–2304.
8. **Griffin DE.** 2003. Immune responses to RNA virus infections of the CNS. Nat. Rev. Immunol. **3**:493–502.
9. **Kumar H, Kawai T, Akira S.** 2009. Pathogen recognition in the innate immune response. Biochem. J. **420**:1–16.
10. **Lee MS, Kim YJ.** 2007. Signaling pathways downstream of pattern-recognition receptors and their cross talk. Annu. Rev. Biochem. **76**:447–480.
11. **Pichlmair A, Reis e Sousa C.** 2007. Innate recognition of viruses. Immunity **27**:370–383.
12. **Binder GK, Griffin DE.** 2003. Immune-mediated clearance of virus from the central nervous system. Microbes Infect. **5**:439–448.
13. **Burdeinick-Kerr R, Wind J, Griffin DE.** 2007. Synergistic roles of antibody and interferon in noncytolytic clearance of Sindbis virus from different regions of the central nervous system. J. Virol. **81**:5628–5636.
14. **Yoneyama M, Fujita T.** 2009. RNA recognition and signal transduction by RIG-I-like receptors. Immunol. Rev. **227**:54–65.
15. **Honda K, Taniguchi T.** 2006. IRFs: master regulators of signalling by Toll-like receptors and cytosolic pattern-recognition receptors. Nat. Rev. Immunol. **6**:644–658.
16. **Wang Y, Swiecki M, McCartney SA, Colonna M.** 2011. dsRNA sensors and plasmacytoid dendritic cells in host defense and autoimmunity. Immunol. Rev. **243**:74–90.
17. **Colonna M, Trinchieri G, Liu YJ.** 2004. Plasmacytoid dendritic cells in immunity. Nat. Immunol. **5**:1219–1226.
18. **Kato H, Sato S, Yoneyama M, Yamamoto M, Uematsu S, Matsui K, Tsujimura T, Takeda K, Fujita T, Takeuchi O, Akira S.** 2005. Cell type-specific involvement of RIG-I in antiviral response. Immunity **23**:19–28.
19. **Cameron JS, Alexopoulou L, Sloane JA, DiBernardo AB, Ma Y, Kosaras B, Flavell R, Strittmatter SM, Volpe J, Sidman R, Vartanian T.** 2007. Toll-like receptor 3 is a potent negative regulator of axonal growth in mammals. J. Neurosci. **27**:13033–13041.
20. **Jackson AC, Rossiter JP, Lafon M.** 2006. Expression of Toll-like receptor 3 in the human cerebellar cortex in rabies, herpes simplex encephalitis, and other neurological diseases. J. Neurovirol. **12**:229–234.
21. **Lafon M, Megret F, Lafage M, Prehaud C.** 2006. The innate immune facet of brain: human neurons express TLR-3 and sense viral dsRNA. J. Mol. Neurosci. **29**:185–194.
22. **McKimmie CS, Fazakerley JK.** 2005. In response to pathogens, glial cells dynamically and differentially regulate Toll-like receptor gene expression. J. Neuroimmunol. **169**:116–125.
23. **Menager P, Roux P, Megret F, Bourgeois JP, Le Sourd AM, Danckaert A, Lafage M, Prehaud C, Lafon M.** 2009. Toll-like receptor 3 (TLR3) plays a major role in the formation of rabies virus Negri Bodies. PLoS Pathog. **5**:e1000315. doi:10.1371/journal.ppat.1000315.
24. **Peltier DC, Simms A, Farmer JR, Miller DJ.** 2010. Human neuronal cells possess functional cytoplasmic and TLR-mediated innate immune pathways influenced by phosphatidylinositol-3 kinase signaling. J. Immunol. **184**:7010–7021.
25. **Prehaud C, Megret F, Lafage M, Lafon M.** 2005. Virus infection switches TLR-3-positive human neurons to become strong producers of β interferon. J. Virol. **79**:12893–12904.
26. **Delhaye S, Paul S, Blakqori G, Minet M, Weber F, Staeheli P, Michiels T.** 2006. Neurons produce type I interferon during viral encephalitis. Proc. Natl. Acad. Sci. U. S. A. **103**:7835–7840.
27. **Roth-Cross JK, Bender SJ, Weiss SR.** 2008. Murine coronavirus mouse hepatitis virus is recognized by MDA5 and induces type I interferon in brain macrophages/microglia. J. Virol. **82**:9829–9838.
28. **Schafer A, Whitmore AC, Konopka JL, Johnston RE.** 2009. Replicon particles of Venezuelan equine encephalitis virus as a reductionist murine model for encephalitis. J. Virol. **83**:4275–4286.
29. **Suthar MS, Ma DY, Thomas S, Lund JM, Zhang N, Daffis S, Rudensky AY, Bevan MJ, Clark EA, Kaja MK, Diamond MS, and Gale M, Jr.** 2010. IPS-1 is essential for the control of West Nile virus infection and immunity. PLoS Pathog. **6**:e1000757. doi:10.1371/journal.ppat.1000757.
30. **Menachery VD, Pasieka TJ, Leib DA.** 2010. Interferon regulatory factor 3-dependent pathways are critical for control of herpes simplex virus type 1 central nervous system infection. J. Virol. **84**:9685–9694.
31. **Zhang SY, Jouanguy E, Ugolini S, Smahi A, Elain G, Romero P, Segal D, Sancho-Shimizu V, Lorenzo L, Puel A, Picard C, Chapgier A, Plancoulaine S, Titeux M, Cognet C, von Bernuth H, Ku CL, Casrouge A, Zhang XX, Barreiro L, Leonard J, Hamilton C, Lebon P, Heron B, Vallee L, Quintana-Murci L, Hovnanian A, Rozenberg F, Vivier E,**

Geissmann F, Tardieu M, Abel L, Casanova JL. 2007. TLR3 deficiency in patients with herpes simplex encephalitis. Science **317**:1522–1527.
32. **Stapleford KA, Rapaport D, Miller DJ.** 2009. Mitochondrion-enriched anionic phospholipids facilitate Flock House virus RNA polymerase membrane association. J. Virol. **83**:4498–4507.
33. **Peng W, Peltier DC, Larsen MJ, Kirchhoff PD, Larsen SD, Neubig RR, Miller DJ.** 2009. Identification of thieno[3,2-*b*]pyrrole derivatives as novel small molecule inhibitors of neurotropic alphaviruses. J. Infect. Dis. **199**:950–957.
34. **Castorena KM, Peltier DC, Peng W, Miller DJ.** 2008. Maturation-dependent responses of human neuronal cells to western equine encephalitis virus infection and type I interferons. Virology **372**:208–220.
35. **Weeks SA, Shield WP, Sahi C, Craig EA, Rospert S, Miller DJ.** 2010. A targeted analysis of cellular chaperones reveals contrasting roles for heat shock protein 70 in Flock House virus RNA replication. J. Virol. **84**:330–339.
36. **Zhang Y, Bhavnani BR.** 2006. Glutamate-induced apoptosis in neuronal cells is mediated via caspase-dependent and independent mechanisms involving calpain and caspase-3 proteases as well as apoptosis inducing factor (AIF) and this process is inhibited by equine estrogens. BMC Neurosci. **7**:49.
37. **Ma W, Tavakoli T, Derby E, Serebryakova Y, Rao MS, Mattson MP.** 2008. Cell-extracellular matrix interactions regulate neural differentiation of human embryonic stem cells. BMC Dev. Biol. **8**:90.
38. **Pankratz MT, Li XJ, Lavaute TM, Lyons EA, Chen X, Zhang SC.** 2007. Directed neural differentiation of human embryonic stem cells via an obligated primitive anterior stage. Stem Cells **25**:1511–1520.
39. **Zhang SC, Wernig M, Duncan ID, Brustle O, Thomson JA.** 2001. In vitro differentiation of transplantable neural precursors from human embryonic stem cells. Nat. Biotechnol. **19**:1129–1133.
40. **Vernon PS, Griffin DE.** 2005. Characterization of an in vitro model of alphavirus infection of immature and mature neurons. J. Virol. **79**:3438–3447.
41. **McJunkin JE, de los Reyes EC, Irazuzta JE, Caceres MJ, Khan RR, Minnich LL, Fu KD, Lovett GD, Tsai T, Thompson A.** 2001. La Crosse encephalitis in children. N. Engl. J. Med. **344**:801–807.
42. **Reisen WK.** 2003. Epidemiology of St. Louis encephalitis virus. Adv. Virus Res. **61**:139–183.
43. **Bowie AG, Unterholzner L.** 2008. Viral evasion and subversion of pattern-recognition receptor signalling. Nat. Rev. Immunol. **8**:911–922.
44. **Randall RE, Goodbourn S.** 2008. Interferons and viruses: an interplay between induction, signalling, antiviral responses and virus countermeasures. J. Gen. Virol. **89**:1–47.
45. **Andersen J, VanScoy S, Cheng TF, Gomez D, Reich NC.** 2008. IRF-3-dependent and augmented target genes during viral infection. Genes Immun. **9**:168–175.
46. **Strauss JH, Strauss EG.** 1994. The alphaviruses: gene expression, replication, and evolution. Microbiol. Rev. **58**:491–562.
47. **Liu WJ, Wang XJ, Clark DC, Lobigs M, Hall RA, Khromykh AA.** 2006. A single amino acid substitution in the West Nile virus nonstructural protein NS2A disables its ability to inhibit α/β interferon induction and attenuates virus virulence in mice. J. Virol. **80**:2396–2404.
48. **Wilson JR, de Sessions PF, Leon MA, Scholle F.** 2008. West Nile virus nonstructural protein 1 inhibits TLR3 signal transduction. J. Virol. **82**:8262–8271.
49. **Aguilar PV, Weaver SC, Basler CF.** 2007. Capsid protein of eastern equine encephalitis virus inhibits host cell gene expression. J. Virol. **81**:3866–3876.
50. **Garmashova N, Atasheva S, Kang W, Weaver SC, Frolova E, Frolov I.** 2007. Analysis of Venezuelan equine encephalitis virus capsid protein function in the inhibition of cellular transcription. J. Virol. **81**:13552–13565.
51. **Garmashova N, Gorchakov R, Volkova E, Paessler S, Frolova E, Frolov I.** 2007. The Old World and New World alphaviruses use different virus-specific proteins for induction of transcriptional shutoff. J. Virol. **81**:2472–2484.
52. **Gorchakov R, Frolova E, Frolov I.** 2005. Inhibition of transcription and translation in Sindbis virus-infected cells. J. Virol. **79**:9397–9409.
53. **Bick MJ, Carroll JW, Gao G, Goff SP, Rice CM, MacDonald MR.** 2003. Expression of the zinc-finger antiviral protein inhibits alphavirus replication. J. Virol. **77**:11555–11562.
54. **Schoggins JW, Wilson SJ, Panis M, Murphy MY, Jones CT, Bieniasz P, Rice CM.** 2011. A diverse range of gene products are effectors of the type I interferon antiviral response. Nature **472**:481–485.
55. **Zhang Y, Burke CW, Ryman KD, Klimstra WB.** 2007. Identification and characterization of interferon-induced proteins that inhibit alphavirus replication. J. Virol. **81**:11246–11255.
56. **Chattopadhyay S, Yamashita M, Zhang Y, Sen GC.** 2011. The IRF-3/Bax-mediated apoptotic pathway, activated by viral cytoplasmic RNA and DNA, inhibits virus replication. J. Virol. **85**:3708–3716.
57. **Eitz Ferrer P, Potthoff S, Kirschnek S, Gasteiger G, Kastenmuller W, Ludwig H, Paschen SA, Villunger A, Sutter G, Drexler I, Hacker G.** 2011. Induction of Noxa-mediated apoptosis by modified vaccinia virus Ankara depends on viral recognition by cytosolic helicases, leading to IRF-3/IFN-β-dependent induction of pro-apoptotic Noxa. PLoS Pathog. **7**:e1002083. doi:10.1371/journal.ppat.1002083.
58. **Heylbroeck C, Balachandran S, Servant MJ, DeLuca C, Barber GN, Lin R, Hiscott J.** 2000. The IRF-3 transcription factor mediates Sendai virus-induced apoptosis. J. Virol. **74**:3781–3792.
59. **Knowlton JJ, Dermody TS, Holm GH.** 2012. Apoptosis induced by mammalian reovirus is β interferon (IFN) independent and enhanced by IFN regulatory factor 3- and NF-κB-dependent expression of Noxa. J. Virol. **86**:1650–1660.
60. **Szretter KJ, Daniels BP, Cho H, Gainey MD, Yokoyama WM, Gale M, Jr, Virgin HW, Klein RS, Sen GC, Diamond MS.** 2012. 2′-O methylation of the viral mRNA cap by West Nile virus evades IFIT1-dependent and -independent mechanisms of host restriction in vivo. PLoS Pathog. **8**:e1002698. doi:10.1371/journal.ppat.1002698.
61. **DeLuca C, Kwon H, Lin R, Wainberg M, Hiscott J.** 1999. NF-κB activation and HIV-1 induced apoptosis. Cytokine Growth Factor Rev. **10**:235–253.
62. **Rolls A, Shechter R, London A, Ziv Y, Ronen A, Levy R, Schwartz M.** 2007. Toll-like receptors modulate adult hippocampal neurogenesis. Nat. Cell Biol. **9**:1081–1088.
63. **Marsh B, Stevens SL, Packard AE, Gopalan B, Hunter B, Leung PY, Harrington CA, Stenzel-Poore MP.** 2009. Systemic lipopolysaccharide protects the brain from ischemic injury by reprogramming the response of the brain to stroke: a critical role for IRF3. J. Neurosci. **29**:9839–9849.
64. **Stevens SL, Stenzel-Poore MP.** 2006. Toll-like receptors and tolerance to ischaemic injury in the brain. Biochem. Soc. Trans. **34**:1352–1355.
65. **Burke CW, Gardner CL, Steffan JJ, Ryman KD, Klimstra WB.** 2009. Characteristics of α/β interferon induction after infection of murine fibroblasts with wild-type and mutant alphaviruses. Virology **395**:121–132.
66. **Pichlmair A, Schulz O, Tan CP, Rehwinkel J, Kato H, Takeuchi O, Akira S, Way M, Schiavo G, Reis e Sousa C.** 2009. Activation of MDA5 requires higher-order RNA structures generated during virus infection. J. Virol. **83**:10761–10769.
67. **Schilte C, Buckwalter MR, Laird ME, Diamond MS, Schwartz O, Albert ML.** 2012. Independent roles for IRF-3 and IRF-7 in hematopoietic and nonhematopoietic cells during host response to Chikungunya infection. J. Immunol. **188**:2967–2971.
68. **White LK, Sali T, Alvarado D, Gatti E, Pierre P, Streblow D, Defilippis VR.** 2011. Chikungunya virus induces IPS-1-dependent innate immune activation and protein kinase R-independent translational shutoff. J. Virol. **85**:606–620.
69. **Blakqori G, Delhaye S, Habjan M, Blair CD, Sanchez-Vargas I, Olson KE, Attarzadeh-Yazdi G, Fragkoudis R, Kohl A, Kalinke U, Weiss S, Michiels T, Staeheli P, Weber F.** 2007. La Crosse bunyavirus nonstructural protein NSs serves to suppress the type I interferon system of mammalian hosts. J. Virol. **81**:4991–4999.
70. **Atasheva S, Fish A, Fornerod M, Frolova EI.** 2010. Venezuelan equine encephalitis virus capsid protein forms a tetrameric complex with CRM1 and importin α/β that obstructs nuclear pore complex function. J. Virol. **84**:4158–4171.
71. **Atasheva S, Garmashova N, Frolov I, Frolova E.** 2008. Venezuelan equine encephalitis virus capsid protein inhibits nuclear import in mammalian but not in mosquito cells. J. Virol. **82**:4028–4041.
72. **Fros JJ, Liu WJ, Prow NA, Geertsema C, Ligtenberg M, Vanlandingham DL, Schnettler E, Vlak JM, Suhrbier A, Khromykh AA, Pijlman GP.** 2010. Chikungunya virus nonstructural protein 2 inhibits type I/II interferon-stimulated JAK-STAT signaling. J. Virol. **84**:10877–10887.
73. **Simmons JD, White LJ, Morrison TE, Montgomery SA, Whitmore AC, Johnston RE, Heise MT.** 2009. Venezuelan equine encephalitis virus disrupts STAT1 signaling by distinct mechanisms independent of host shutoff. J. Virol. **83**:10571–10581.
74. **Simmons JD, Wollish AC, Heise MT.** 2010. A determinant of Sindbis virus neurovirulence enables efficient disruption of Jak/STAT signaling. J. Virol. **84**:11429–11439.
75. **Yin J, Gardner CL, Burke CW, Ryman KD, Klimstra WB.** 2009. Similarities and differences in antagonism of neuron α/β interferon responses by Venezuelan equine encephalitis and Sindbis alphaviruses. J. Virol. **83**:10036–10047.